Understanding fracture of a carbon black filled rubber compound using material force theory

Understanding fracture of a carbon black filled rubber compound using material force theory

Anand Poomuthu[a,*], Radek Stoček[b,c], Santanu Chattopadhyay[a], Dipak Khastgir[a], Michael Kaliske[d], Kaan Ozenę[d], Priyanka Sekar[a]

[a]*Rubber Technology Center, Indian Institute of Technology Kharagpur, India*

[b]*Centre of Polymer Systems, Tomas Bata University in Zlin, Zlin, Czech Republic*

[c]*PRL Polymer Research Lab, Zlin, Czech Republic*

[d]*Institute for Structural Analysis, Technische Universitdt Dresden, Dresden, Germany*

[*]*Corresponding author. E-mail address: anandpoomuthu3@gmail.com (A. Poomuthu).*

ABSTRACT

This paper is based on the determination of important fracture parameters for commercially important rubber blends through experimental and finite element modeling methods. Properties of NR/BR blends, which are mainly suitable for tire applications, of various compositions have been tested under tensile load and the result is utilized to determine the suitable hyperelastic material model. A model proposed by Yeoh has been found to be more relevant to the test materials and is used to represent them in simulation. Single Edge Notched Tensile samples (SENT) are ued for the fracture analysis. The samples are tested for uniaxial Mode I fracture (Tensile), which is the most commonly observed among the three modes of fracture, and crack growth was studied using the Virtual Crack Closure Technique (VCCT). A finite-element replica of the test specimen has been created using in-house code, which uses an implicit mesh adaptive method to study the strain potential around the crack tip. The code for each specimen is executed using the commercially available third-party software ANSYS Parametric Design Language (APDL). The stress-strain behaviors from experimental and simulation responses were compared. The energy release rate otherwise known as tearing energy has been derived for both experimental and numerical tests.

Keywords: Hyperelastic, tearing energy, material force, virtual crack closure

1. Introduction

Knowledge of the mode of failure is essential for any material being employed for high-performance applications. For conventional structural materials such as metals, concrete, and their composites, the fracture behavior has been extensively studied [**1**]. These materials have high modulus and show small strain when subjected to different stresses. In the case of polymers, especially elastomers, studying fracture behavior is tedious, as these materials exhibit very high levels of deformation even for minimal

amounts of applied load. These large deformations make the choice of the appropriate instrument to measure stress at very low strain difficult. These materials also tend to buckle under compressive loads. Hence, their study is limited to only two modes of deformation, either by quasi-static loading, which is time-dependent but slow enough that internal thermodynamic effects can be ignored, or by dynamic loading.

The stress concentration around a circular hole in a plate was calculated by Inglis [**2**] (1913), who found it to be of much higher magnitude than the nominal stress. Griffith [**3**] (1921) presented the fracture stress for a glass fiber as a function of its diameter and proposed that the difference between theoretical and experimental stress arises due to the presence of defects. This work is considered to have originated the discipline of fracture mechanics.

Rivlin's Phenomenological Theory of Rubber Elasticity was based on the concept that the material is isotropic in nature and its elastic properties can be presented in terms of a strain-energy function, 'W'. Rivlin and Thomas [**4**] (1953) demonstrated strain energy density to be the driving parameter of crack growth in an elastomeric structure, and proposed the following expression for its experimental calculation:

$$T = -\frac{\partial W}{\partial A} \tag{1}$$

where T is the tearing energy, W is the strain energy and A is the interfacial area of the grown crack. Thomas [**5**] (1955) further clarified that the key fracture property, i.e., strain energy density, is a characteristic of the material itself and largely independent of the test piece geometry, after studying various types of specimens such as single edge notched tensile specimens (SENT), plane shear specimens, etc.

Knowles and Sternberg [**6,7**] carried out a lowest-order asymptotic analysis of the deformations and stresses near the tip of a traction-free crack in an elastic slab of all-around infinite extent, which - at infinity -is subjected to uniform uni-axial tension at right angles to the crack faces.

Since fracturing is represented as a function of energy, a number of models have been presented by various researchers using strain energy density as a function of principal strain invariants. These models are known as hyperelastic material models. The earliest of them is the Rivlin model, which considers ' W as the sum of the product of the first two strain-invariant terms. The most common mode of fracture observed in structures is the tensile or opening mode. Hence Yeoh [**7**] (1990) suggested a model that assumed ' W' to be a function of the strain invariants of the uniaxial tensile mode alone. Such a model simplified the problem of determining material coefficients and provided a method for determining these coefficients from simple tensile stress-strain data.

$$W = \sum_{I,J=0}^{n} C_{10}(I_1 - 3) + C_{20}(I_1 - 3)^2 + C_{30}(I_1 - 3)^3 \tag{2}$$

Ihueze and Mgnomena [**8**] (2014) studied three different types of hyperelastic material models - the Arruda-Boyce model, the Mooney-Rivlin model, and the 3rd order Yeoh model - to represent the uniaxial tensile behavior of NR filled with modified Kaolin. Among these models, the Yeoh model was

found to exhibit the best fit. Ghosh. P [**9**] (2003) used the 3rd order Yeoh model for rubber suitable for tire applications to predict rolling resistance.

As mentioned earlier, the difference between the theoretical and experimental fracture behavior arises due to the presence of flaws, such as contaminations, micro-cracks, or dislocations, present in the structure. In order to compute the behavior precisely, one has to consider these flaws in the model without fail. Typically, these cracks are approached as discrete discontinuities in the structure. They can be represented by various methods such as node duplication by mesh adaptation, displacement field enrichment using discontinuities, and the phase-field model, where the discontinuity is introduced at the continuum level rather than at the structural level.

The concept of physical forces was in the past successfully used to describe the stress-strain behavior of the structure being studied. When discontinuities are included in the structure, however, physical forces alone can no longer describe the behavior and the results are left with errors. These errors must be kept as small as possible. Eshelby [**10**] (1951) introduced the concept of forces acting on an elastic singularity. These are thermodynamic driving forces on any kind of inhomogeneities and discontinuities in a structure. At the crack tip, the material force can be understood as the force preventing the crack to vary its position under existing loading conditions, which the crack would otherwise do in order to reach a neighboring state that is energetically more advantageous.

Maugin and Trimarco [**11**] (1992) proposed a material force framework for fractures in an inelastic material. Meuller [**12**] (2002) et al. demonstrated how configurational forces can be used to check and improve finite element solutions. Ozenę and Kaliske [**13**] (2014) outlined a general r-adaptive model for rate-dependent crack propagation in rubbery polymers at finite strains and discussed its numerical implementation. With a suitable numerical example, they showed that the material force approach successfully evaluates the energy release rate obtained by experimental study of a hyperelastic material.

This paper presents the experimental determination of energy release rate under quasi-static loading for neat natural rubber compounds, neat polybutadiene rubber compounds, and their blends, suitable for tire tread applications, with varying carbon black loading. A computed replica of the sample is designed using the Yeoh model and material force values are used, via suitable post-processing steps, to determine the energy release rate equivalents through the virtual crack closure technique (VCCT). The experimental and simulated results are compared using the material force and the influence of major compounding parameters (blend ratio and carbon black loading) is discussed.

2. Experimental

2.1. Materials

Compound mixing was done in a laboratory internal mixture. Constant viscosity natural rubber (CV60) and Polybutadiene rubber (Buna CB 24) were used in this study. All compounds were filled with N339 HAF-HS carbon black, widely used in tire applications. Compounds were crosslinked using an EV curing system with sulphur as the curing agent and Vulkacit CZ (N-cyclohexyl-2-benzothiazolesulfe-namide) as the sole accelerator. Vulkanox 4010 (N-Isopropyl-N'-phenyl-p-phenylenediamine), commonly known as IPPD, was used as antioxidant. Table 3 presents the detailed formulation of compounds used in the study.

The curing characteristics of the compounds were tested using an MDR 3000 Rheometer; results are given in Table 4 as support data.

2.2. Determination of material parameters

Three units each of dumbbell-shaped samples of type S2 were prepared from the cured sheets of compounds. The samples were tested for uniaxial tensile loading using a TESTOMETRIC M350 - 5CT universal tensile testing machine at a loading speed of 100 mm/min, where the unstrained length between the clamps was 30 mm. From the measured force-displacement data, the stress-strain relation was derived for each material.

Actual stress-strain curves from this experiment were compared against theoretical counterparts from various material models, especially hyperelastic models. After a detailed study, it was found that the material behavior fits well with the 3rd order Yeoh hyperelastic model.

Fig. 1a & b show the comparison of experimental stress-strain behavior of NR filled with 40 phr of carbon black and crosslinked by an efficient curing system, with predictions of some of the existing hyperelastic material models such as Mooney-Rivlin, Neo-Hookean, Yeoh, Arruda-Boyce, and Ogden [**13**]. Among the existing models, it is clear that the experimental material behavior is close to that of the 3rd order Yeoh model, implying that this model would require the least effort to fit experimental data.

An in-house tool developed at the Institute for Statics and Dynamics of Structures was used to determine the material parameters corresponding to the 3rd order Yeoh model, C_{10}, C_{20}, C_{30}, d_1, d_2, and d_3. The model is based on a linear least squares problem and solved by singlevalue decomposition.

From the experimental data, material parameters were derived using the linear least squares method. First, the simulated stress is calculated as the derivative of the Yeoh strain energy function with respect to strain. This is a linear polynomial expression with the unknown parameters (C1, C2, C3). When this polynomial is written down in matrix notation, one obtains:

$$\begin{bmatrix} X_{11} & X_{12} & X_{13} \\ X_{21} & X_{22} & X_{23} \\ X_{31} & X_{32} & X_{33} \end{bmatrix} \begin{bmatrix} C_1 \\ C_2 \\ C_3 \end{bmatrix} \qquad (3)$$

$$\begin{bmatrix} X_{m1} & X_{m2} & X_{m3} \end{bmatrix}$$

Then, the sum of the squares of the differences between the simulated values (X C) and the measured stresses (Y) is minimized subject to $(Y - X C)^2 > \min$. The normal equation $(X^T X)\, C = X^T Y$ is obtained by this approach. This normal equation can now be solved by single-value decomposition to obtain the result vector [C1, C2, C3], whose elements are the Yeoh Parameters.

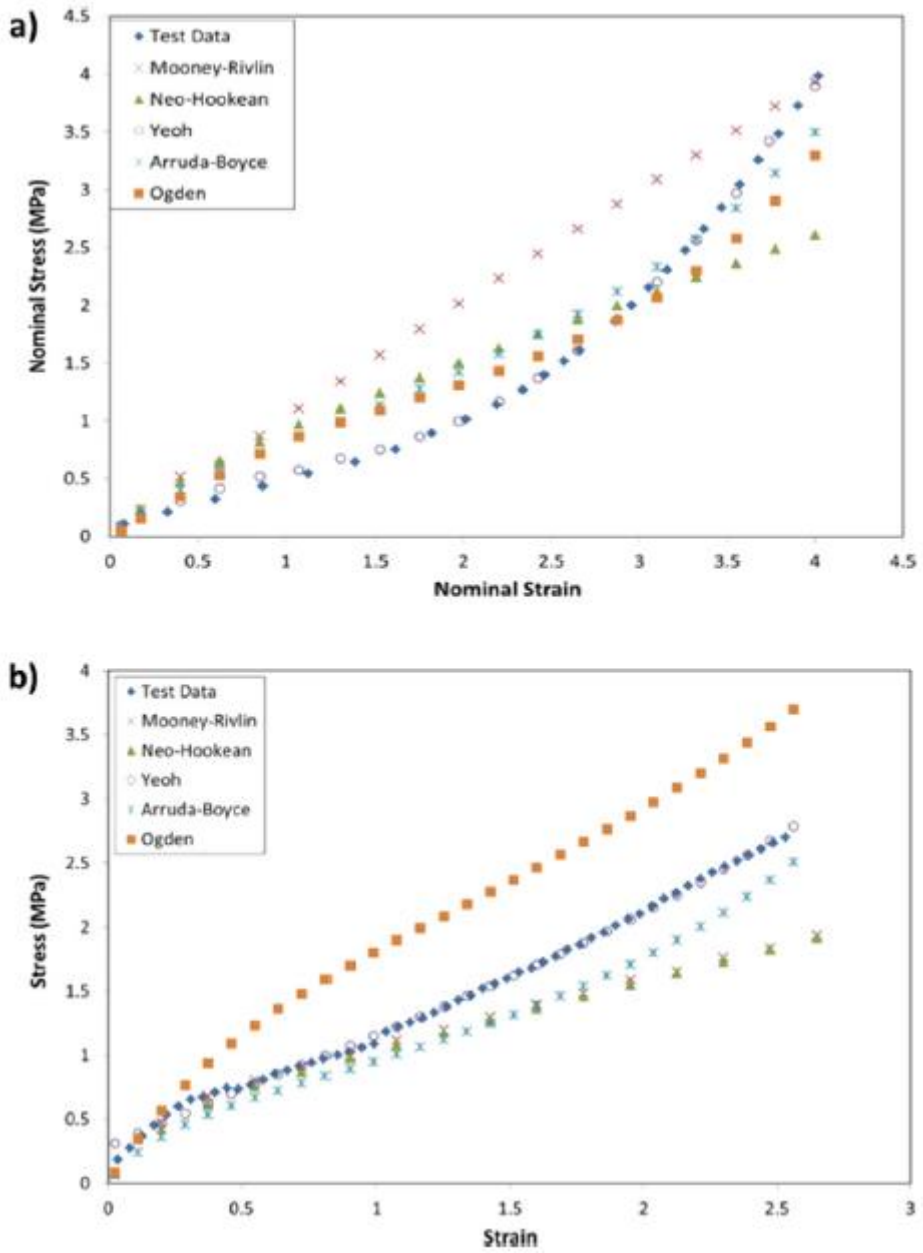

Fig. 1. (a) Uniaxial and (b) biaxial tension of filled NR and some hyperelastic models.

2.3. Study of crack growth under quasi-static loading

Fracturing under quasi-static loading was tested with a TESTOME-TRIC M350 - 5CT universal tensile testing machine. SENT specimens of each compound were used for the study. The sample is a rectangular strip of dimensions 10 mm x 30 mm x 2.1 mm (width x length between clamps x thickness), which has a notch of length 1.5 mm starting from one edge of its vertical midpoint. The length as well as the exact orthogonal position of the notch to the long axis of the specimen is controlled by a precision notching device, which ensures reproducibility of the notch feature. A graphic representation of the sample is given in **Fig. 2**a. Testing is performed with conventional tensile grips at the rate of 100 mm/min. The sample was stressed until complete rupture and force-displacement data was collected using a supplier-provided user interface. Instantaneous pictures of the crack were captured using an Imaging Sense DMK42BUC03 industrial camera at 40 fps.

2.4. Simulation of crack growth

A replica of the sample being actually stressed (excluding the gripped portions) is generated using the commercially-available third-party software ANSYS APDL. The input code for this program was written in-house. All sample descriptors such as dimensions, hyperelastic material properties, element type and number, mesh, crack details, boundary conditions, and loads were input in their respective stages (pre-processing or solution). The crack type and definitions were introduced using special contour integral (CINT) commands. Elements around the crack tip were redefined using an adaptive method. The redefined mesh structure around the crack tip in a SENT specimen, along with the specimen being studied, is shown in **Fig. 2**c.

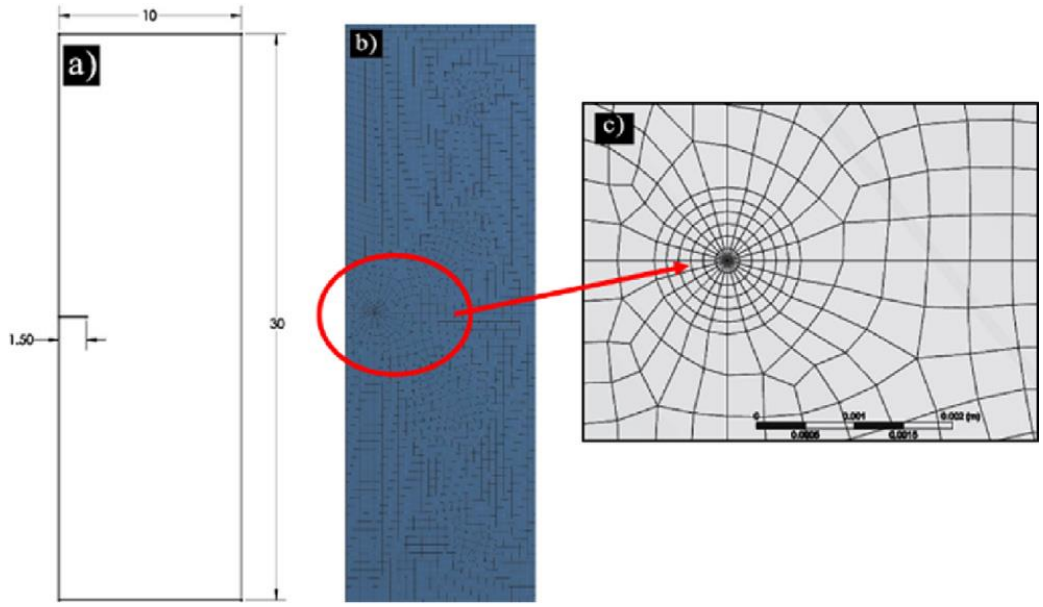

Fig. 2. (a) SENT specimen (b) Mesh structure of SENT specimen (c) Redefined mesh around crack tip.

In the post-processing stage, the expected result parameters such as the J-integral and material force, as well as functions for the acquisition of underlying data, are defined. The code was executed in the user interface and repeated if preliminary outputs did not converge. The virtual crack closure technique, which is shown in the **Fig. 3**, was used to determine the strain energy density from one discrete strain level to another.

3. Results and discussion

3.1. Determining material model & its parameters

The choice of material model is the principal task and can be done with simple tensile stress-strain data. Other test methods such as uniaxial compression and biaxial tension could provide more precise data on the behavior of the material, but are not taken into account here, as the focus is primarily on the opening mode of crack propagation.

Fig. 4 represents typical stress-strain behavior of neat natural rubber, neat polybutadiene rubber, and their blends. The plot clearly demonstrates the impact of blending and the influence of filler content in the compound.

As expected, NR and BR exhibit similar tensile patterns, with NR showing the highest elongation at break and tensile strength.

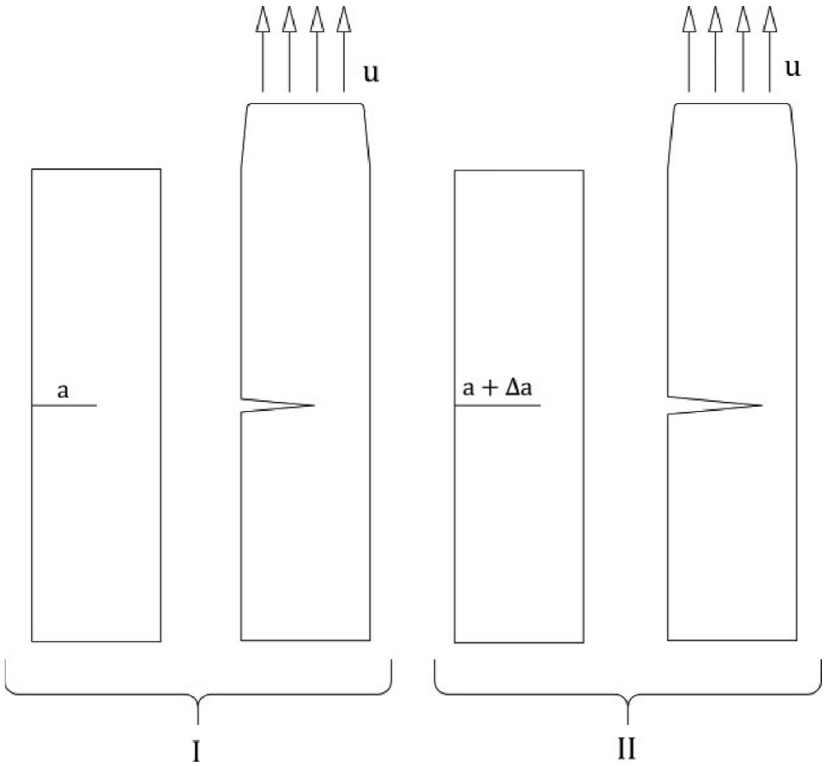

Fig. 3. Virtual crack closure technique.

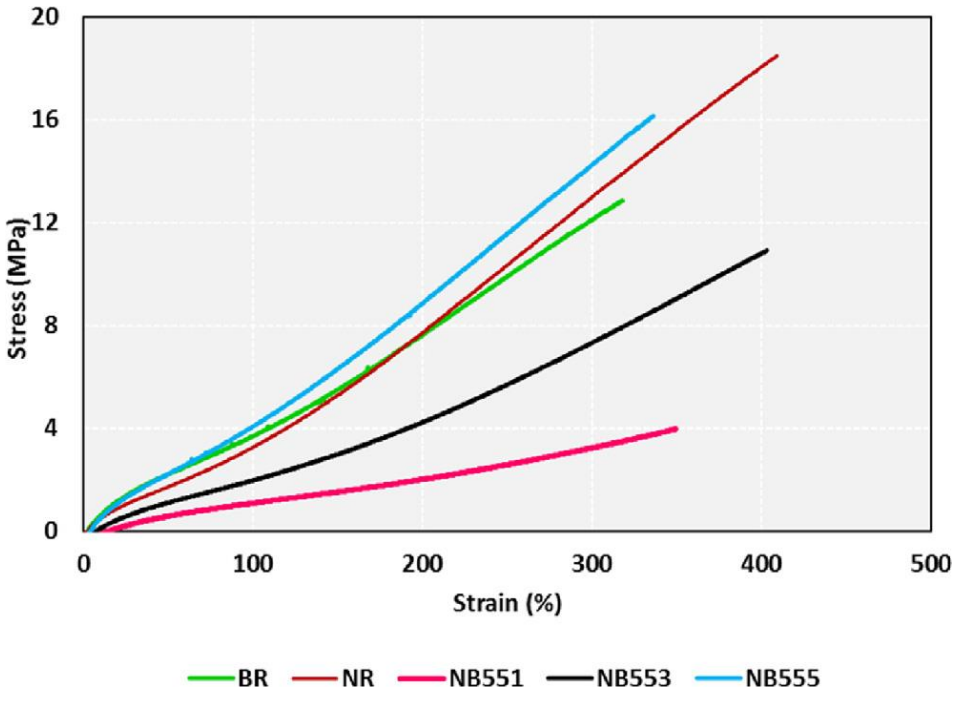

Fig. 4. Stress-Strain Behavior of NR, BR, and their blends.

The modulus changes after blending with BR but increases proportionately with the filler content. The modulus of the blend compound is lower than the neat rubber compound as the molecular symmetry which leads to strain-induced crystallization, especially in NR, is disturbed by blending.

At the same time, increasing the amount of reinforcing filler from 10 phr to 30 phr and 50 phr imparts more rigidity to the compound through restriction of chain mobility and hence the modulus steadily increases. After fitting the experimental stress-strain data to the proposed model, its material parameters were determined by the procedure mentioned earlier. The calculated material constants for each compound are given in **Table 1**.

The incompressibility parameters d_1, d_2, and d_3 were found to be 0 for all compounds. Still, they cannot be ignored while assigning material features through the parametric language.

3.2. Fracture experiment under quasi-static loading

The crack development pattern in SENT specimen of NR, BR, and their blend under quasi-static load is presented in the **Fig. 5**. These pictures particularly represent SENT samples from the fracturing experiment at various levels of strain up to failure, considering total rupture as 100% strained. In that perspective, the images from left to right represent samples at strain levels of 0-10%, 40-60%, and 90-100%, respectively.

NR Specimen shows a non-linear crack pathway, which indicates the extent of resistance offered by the material to the development of a crack. The well-known phenomenon of strain-induced crystallization prevents the crack from slipping past the polymer chain and the process is ultimately delayed.

In contrast, BR shows an almost linear path of failure. The failure pattern is similar to brittle failure observed in rigid plastics and metals. The time until failure is also much less than for NR. The strain-induced crystallization behavior is almost absent in BR compounds at ambient temperature, as the crystalline melting temperature of BR is 4 °C. There is also appreciable cis-trans isomerization in BR compounds during vulcanization leading to heterogeneity of the microstructure. This adversely affects strain-induced crystallization [**15,16**].

Table 1 Material parameters from experiment as coefficients for the 3rd order Yeoh model.

Material	C_{10}	C_{20}	C_{30}	d_1	d_2	d_3
NR	1.220	$1.22 * 10^{-5}$	$7.24 * 10^{-9}$	0	0	0
NB551	0.349	$5.53 * 10^{-3}$	$-3.25 * 10^{-5}$	0	0	0
NB553	0.480	0.021	$-2.28 * 10^{-4}$	0	0	0
NB555	1.000	0.008	$-8.46 * 10^{-6}$	0	0	0
BR	0.946	0.034	$-5.86 * 10^{-4}$	0	0	0

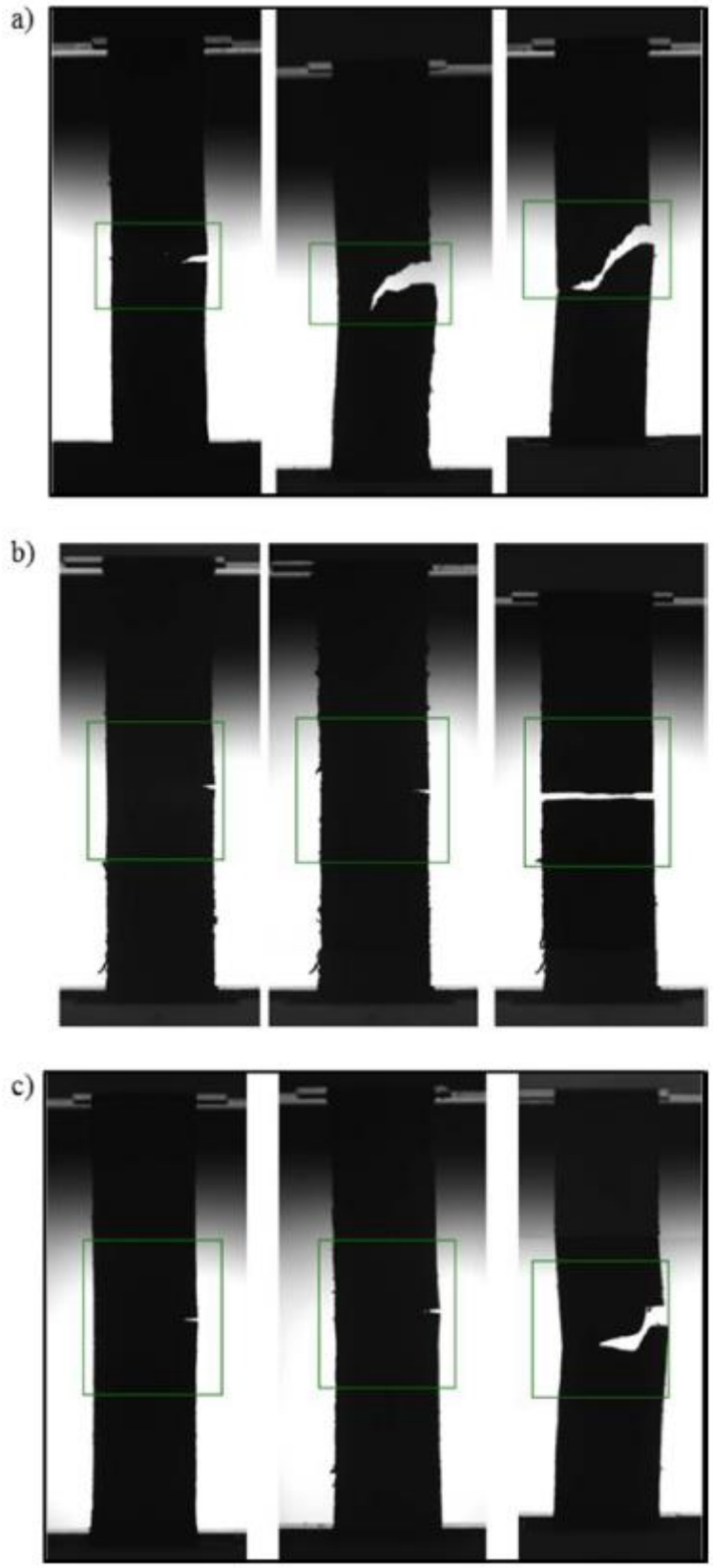

Fig. 5. Crack development in SENT specimen of (a) NR (b) BR (c) NB555.

It has been observed in the literature that not only BR, but also many other synthetic rubbers show similar behavior. This convincingly demonstrates the fact that natural rubber has more crack propagation resistance than synthetic rubbers. The failure behavior for the blended sample is a

combination of the effects seen in both NR and BR. The failure pattern is very similar to that of NR, whereas time to failure is much shorter than in NR.

This implies that blending with BR reduces the crack propagation resistance of NR, especially in carbon black filled compounds. This may be due to the reinforcing effect of the filler, which is more prominent in BR compared to that in NR [**17-19**]. The stress-strain behavior for each sample can be used to determine their experimental energy release rate or tearing energy. The area under the graph represents the tearing energy, which is the energy absorbed by the material throughout the cycle or, in other words, the minimum amount of energy required for rubber chain breakage.

As expected based on the literature, [**21**] this minimum tearing energy of notched samples is much higher for NR than for BR, whereas in a similar experiment performed with a notch-free sample, the opposite result may well have been observed.

3.3. Fracture simulation and estimation of material force

The design language executes the tensile stretching of a given specimen under the described loading and boundary conditions. During post-processing steps, the crack environment is well defined and the growth characteristics are captured using **Get* and *Stat functions. Here, the solver "**Get*" retrieves a value and stores it as a scalar parameter or part of an array parameter whereas "**Stat*" is used to list the retrieved parameters in the output summary.

The direction and path of crack growth are not considered in this paper. The sum of reaction forces from each surface element is generated through an offset point, from which force-displacement data for the entire specimen are obtained.

Another post-processing step, **Mfor*, defines the material force vector and the result is obtained as a convergent solution by contour-integrating the force vectors around the crack tip. The negative sign indicates the direction of material force is opposite to the crack growth direction, which follows from the definition of material force.

Fig. 6 depicts the maximum principal strain observed in a SENT specimen around the crack tip when subjected to a displacement of 5 mm. This behavior is commonly exhibited by all the compounds studied, irrespective of their nature.

Experimental and simulated results of tensile behavior were compared and found to be almost identical. **Fig. 7**a & b represent the above for neat NR and BR compounds, whereas **Fig. 7**c represents the same for NR/BR blends with various loadings of carbon black. The simulated results are capable of replicating all their respective experimental counterparts.

The close fit validates the ability of the 3rd order Yeoh model to represent the material of interest. The simulated data captures all available compound variations such as the impact of blending and extent of filler loading. Based on this satisfactory performance, we decided to proceed with an energy-based approach using this model to understand the fracture.

The energy release rates obtained from the experimental as well as the simulated data and the material force vector values for the respective compounds are compared against each other in **Table 2**. The material force value presented is the sum of magnitudes of vectors around the crack tip.

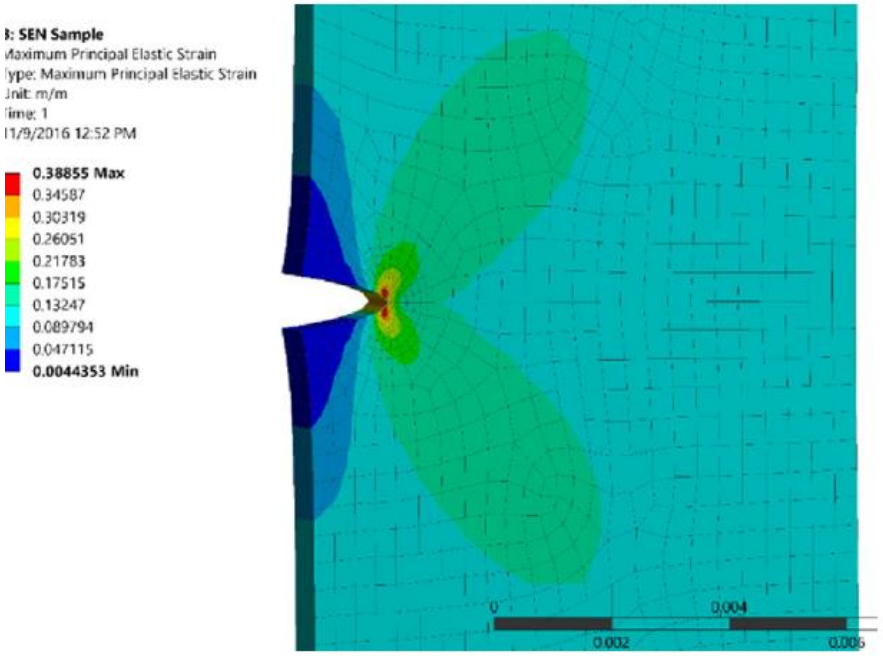

Fig. 6. Maximum principal strain around the crack tip in a SENT specimen.

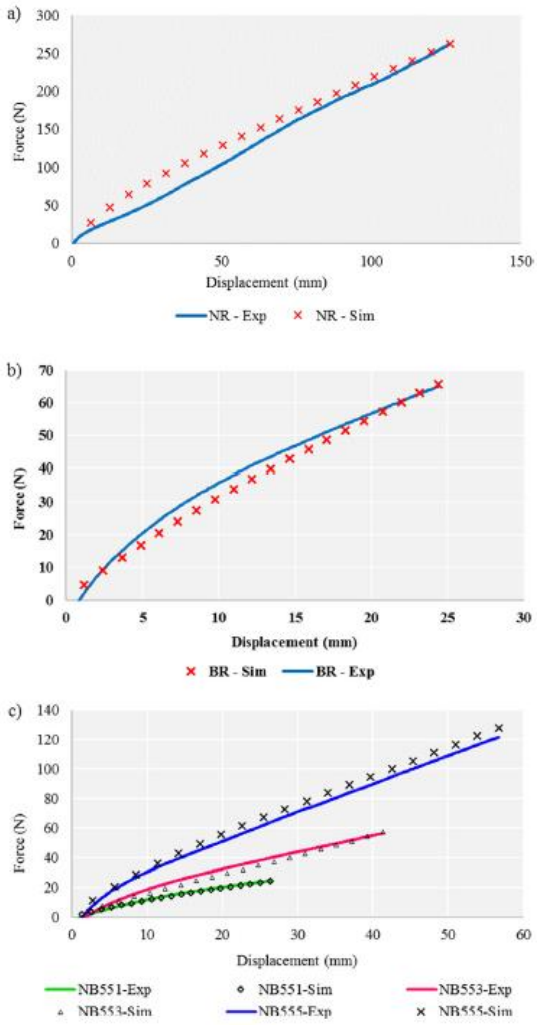

Fig. 7. Tensile response data of (a) neat NR, (b) neat BR, (c) NR/BR blends with increasing carbon black content.

Table 2 Energy release rate and Material force for experimental and simulated tensile testing of a SENT specimen.

Sample	Energy release rate			Material force (J/m^2)
	Experimental (J/m^2)	Simulated (J/m^2)	Difference (%)	
NR	804.6	880.0	8.6	879.7
NB551	16.2	17.0	4.7	18.1
NB553	57.2	57.5	0.5	43.9
NB555	168.0	188.4	10.8	199.3
BR	40.2	41.1	2.2	44.0

The energy release rates were found to be close for all compounds except for NB555 (~11% difference between experimental and simulated results). Such a difference is unsurprising in this compound, as it has the maximum possible variation with respect to blend ratio (50/ 50), which affects the molecular regularity to a large extent and leads to a more random fracturing behavior. According to the material force approach proposed, the energy release rate is equivalent to the material force. Hence, the material force can be used as a single parameter to study fracturing of structures. However, this may be different for time-dependent loading. The nature of such a parameter under various strain rates and the influence of different waveforms are to be examined in detail in a future work.

4. Summary & conclusion

An experiment was conducted to characterize the fracture behavior of natural rubber (NR), polybutadiene rubber (BR), and their blends with 10 phr, 30 phr, and 50 phr of carbon black loading. The quasistatic tensile fracture tests were performed using a Universal Testing Machine (UTM) for single-edge-notched tensile test specimens.

In order to determine the crack driving force, finite elemental analysis (FEA) was done with the hyperelastic material properties of the neat rubbers and their binary blends. A constitutive equation framed by Yeoh was used to represent the hyperelastic behavior of the material. Material parameters were determined using a simple tensile test method.

The experimental and finite element analysis results of quasi-static fracture tests were compared and found to be more or less similar. The existing fracture parameters were compared against a new parameter, which is a configurational force. As both existing and new fracture terms were found similar, the new approach is put forward as a one-step solution to analyze the fracture using finite element modeling.

References

[1] T.L. Anderson, Fracture Mechanics: Fundamentals and Applications, CRC Press, 2005, pp. 219-254 ISBN: 9780429125676.

[2] C.E Inglis, I.N.A.Trans. 55(1) (1913) 219-240.

[3] A.A. Griffith, Philosoph. Trans. Roy. Soc. London A 221 (1921) 163-198, **https://doi.org/10.1098/rsta.1921.0006**.

[4] R.S. Rivlin, A.G. Thomas, J. Polym. Sci. X (3) (1953) 309, **https://doi.org/10.1002/ pol.1953.120100303**.

[5] A.G. Thomas, J. Polym. Sci. XVIII (1955) 177-188, **https://doi.org/10.1002/pol. 1955.120188802**.

[6] J.K. Knowles, E. Sternberg, J. Elast. 3 (2) (1973) 67-107, **https://doi.org/10.1007/ BF00045816**.

[7] J.K. Knowles, E. Sternberg, J. Elast. 4 (3) (1973) 201-233, **https://doi.org/10. 1007/BF00049265**.

[8] O.H. Yeoh, Rubber Chem. Technol. 66 (1993) 760, **https://doi.org/10.5254/1. 3538343**.

[9] C.C. Ihueze, C.O. Mgnemena, J. Sci. Res. Rep. 3 (19) (2014), **https://doi.org/10. 9734/JSRR/2014/11587**.

[10] P. Ghosh, A. Saha, R. Mukhopadhyay, Constitutive models for Rubbers III, 2003, pp. 141-146. ISBN: 9058095665.

[11] J.D. Eshelby, Philosoph. Trans. Roy. Soc. LondonA 244 (1951) 87-112, **https://doi. org/10.1098/rsta.1951.0016**.

[12] G.A. Maugin, C. Trimarco, Acta Mech. 94 (1997) 1-28, **https://doi.org/10.1007/ BF01177002**.

[13] R. Mueller, S. Kolling, D. Gross, Int. J. Num. Meth. Eng. 53 (2002) 1557-1574, **https://doi.org/10.1002/nme.351**.

[15] M. Shahzad, Mat. Res. 18 (5) (2015) 918-924, **https://doi.org/10.1590/1516-1439.320414**.

[16] Edward F. Devlin, Rub. Chem. And Tech. 59 (4) (1986) 666-670, **https://doi.org/ 10.5254/1.3538227**.

[17] I.Y. Poddubnyi, Poly. Sci. U.S.S.R. 10(6) (1968) 1603-1612. **https://doi.org/10. 1016/0032-3950(68)90023-3**.

[18] W.E. Hess, Rub. Chem. Tech. 58(2) (1985) 350-382. **https://doi.org/10.5254/1. 3536071**.

[19] W.M. Hess, Rub. Chem. Tech. 50(2) (1977) 301-326. **https://doi.org/10.5254/1. 3535145**.

[21] H.J. Chiu, J. Mat. Eng. Perf. 15 (2006) 88-94, **https://doi.org/10.1361/ 105994906X83448**.

Further reading

[14] K. Ozenę, M. Kaliske, Int. J. Numer. Meth. Eng. 100 (2014) **669-670, https://doi. org/10.1002/nme.4774**.

[20] G.R. Hamed, Rub. Chem. Tech. 69(5) (1996) 807-818. **https://doi.org/10.5254/1. 3538404**.

[22] A.N. Gent, P.B. Lindley, A.G. Thomas, J. Poly. Sci. 8 (1964) 455-466, **https://doi.org/10.1002/app.1964.070080129**.

[23] R. Stoček, Adv in Poly. Sci., Springer New York LLC, 2017, pp. 361-398. **https://doi.org/10.1007/978-3-319-47696-4**.

[24] W.V. Mars, C. Kipscholl, R. Stocek, Intirnsic strength analyzer based on cutting method, in: 190th Technical Meeting of the Rubber, ACS, Pittsburgh, PA, October 10-13, 2016, ISSN: 1547-1977.